Available online at www.sciencedirect.com
SCIENCE DIRECT
Biochimica et Biophysica Acta 1701 (2004) 49–59
BIOCHIMICA ET BIOPHYSICA ACTA
BBA
www.bba-direct.com

Probing a hydrogen bond pair and the FAD redox properties in the proline dehydrogenase domain of *Escherichia coli* PutA

Berevan A. Baban[a,1], Madhavan P. Vinod[a,b], John J. Tanner[c,d], Donald F. Becker[a,b,*]

[a] *Department of Chemistry and Biochemistry, University of Missouri-St. Louis, St. Louis, MO 63121, USA*
[b] *Department of Biochemistry, Redox Biology Center, University of Nebraska, Lincoln, NE 68588-0664, USA*
[c] *Department of Chemistry, University of Missouri-Columbia, Columbia, MO 65211, USA*
[d] *Department of Biochemistry, University of Missouri-Columbia, Columbia, MO 65211, USA*

Received 25 February 2004; accepted 4 June 2004
Available online 2 July 2004

Abstract

The PutA flavoprotein from *Escherichia coli* combines DNA-binding, proline dehydrogenase (PRODH), and Δ^1-pyrroline-5-carboxylate dehydrogenase (P5CDH) activities onto a single polypeptide. Recently, an X-ray crystal structure of PutA residues 87–612 was solved which identified a D370–Y540 hydrogen bond pair in the PRODH active site that appears to have an important role in shaping proline binding and the FAD redox environment. To examine the role of D370–Y540 in the PRODH active site, mutants D370A, Y540F, and D370A/Y540F were characterized in a form of PutA containing only residues 86–601 (PutA86–601) designed to mimic the known structural region of PutA (87–612). Disruption of the D370–Y540 pair only slightly diminished k_{cat}, while more noticeable affects were observed in K_m. The mutant D370A/Y540F showed the most significant changes in the pH dependence of k_{cat}/K_m and K_m relative to wild-type PutA86–601 with an apparent pK_a value of about 8.2 for the pH-dependent decrease in K_m. From the pH profile of D370A/Y540F inhibition by L-tetrahydro-2-furoic acid (L-THFA), the pH dependency of K_m in D370A/Y540F is interpreted as resulting from the deprotonation of the proline amine in the E–S complex. Replacement of D370 and Y540 produces divergent effects on the E_m for bound FAD. At pH 7.0, E_m values of -0.026, -0.089 and -0.042 V were determined for the two-electron reduction of bound FAD in D370A, Y540F and D370A/Y540F, respectively. The 40-mV positive shift in E_m determined for D370A relative to wild-type PutA86–601 ($E_m = -0.066$ V, pH 7.0) indicates D370 has a key role in modulating the FAD redox environment.

Keywords: Proline dehydrogenase; FAD redox potential; Active site residue

1. Introduction

Proline is involved in various processes such as colonization of the rhizophere, osmotic regulation in bacteria, stress tolerance in plants, programmed cell death, and mitochondrial oxidative metabolism [1–6]. The catabolic processing of proline to glutamate is achieved in two oxidative steps by the coordinated actions of proline dehydrogenase (PRODH) and Δ^1-pyrroline-5-carboxylate dehydrogenase (P5CDH) [7–10]. In the first step (see Fig. 1), PRODH catalyzes the transfer of two electrons from proline to a tightly associated FAD prosthetic group to generate Δ^1-pyrroline-5-carboxylate (reductive half-reaction). The two electrons from reduced FAD are then transferred to the electron transport chain to complete the catalytic cycle (oxidative half-reaction). The second step involves hydrolysis of Δ^1-pyrroline-5-carboxylate to glutamate-γ-semialdehyde and subsequent transfer of two electrons to an NAD^+ cofactor by P5CDH to yield glutamate. Deficiencies in PRODH and P5CDH in humans result in type I and type II hyperprolinemia, respectively [11–13].

Abbreviations: FAD, flavin adenine dinucleotide; *put*, proline utilization; NAD^+, nicotinamide adenine dinucleotide; PRODH, proline dehydrogenase; P5CDH, Δ^1-pyrroline-5-carboxylate dehydrogenase; P5C, Δ^1-pyrroline-5-carboxylate; THFA, tetrahydro-2-furoic acid; DCPIP, dichlorophenolindophenol; EDTA, ethylenediaminetetraacetic acid; SDS-PAGE, sodium dodecyl sulfate polyacrylamide electrophoresis; E_m, midpoint potential

* Corresponding author. Department of Biochemistry, Beadle Center, University of Nebraska, Lincoln, NE 68588-0664, USA. Tel.: +1-402-472-9652; fax: +1-402-472-7842.
E-mail address: dbecker3@unl.edu (D.F. Becker).
[1] Present address: Department of Anatomy and Neurobiology, Washington University School of Medicine, 660 South Euclid Avenue, Campus Box 8108, St. Louis, Missouri 63110, USA.

1570-9639/$ - see front matter © 2004 Elsevier B.V. All rights reserved.
doi:10.1016/j.bbapap.2004.06.001

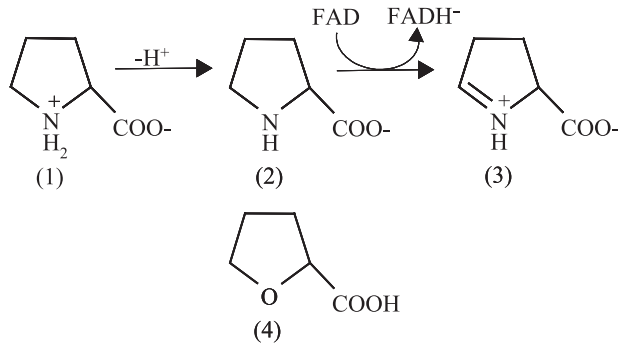

Fig. 1. Reductive half-reaction catalyzed by the PRODH domain showing the zwitterionic (1) and anionic (2) forms of proline and the product, Δ^1-pyrroline-5-carboxylate (3). Tetrahydro-2-furoic acid (4), a competitive inhibitor of PRODH activity, is also shown.

In bacteria, PRODH and P5CDH activities are combined on the bifunctional proline utilization A (PutA) flavoprotein, which is encoded by the *putA* gene [8–10]. PutA has also been shown to have DNA-binding activity and act as an autogeneous transcriptional repressor of the *putP* and *putA* genes of the proline utilization (*put*) regulon in *Escherichia coli* and *Salmonella typhimurium* [9,14–17]. The *putP* gene encodes the PutP high affinity Na^+-proline transporter [18]. The regulation of the *put* genes in *E. coli* and *S. typhimurium* depends on the availability of L-proline and the intracellular location of PutA. In the absence of proline, PutA accumulates in the cytoplasm and represses transcription of the *put* genes by binding to promoter sequences in the *put* control intergenic DNA region [9,17]. In the presence of proline, PutA shifts from the cytoplasm to the membrane activating transcription of the *put* genes and proline oxidation [19–22].

PutA from *E. coli*, the subject of this study, is a polypeptide of 1320 amino acids that purifies as a dimer and contains one noncovalently bound FAD per monomer [9,23]. Previously, a truncated PutA protein from *E. coli* that contains residues 1–669 (PutA669) was shown to have PRODH and DNA-binding activities but lack P5CDH activity [24]. More recently, the X-ray crystallographic structure of PutA669 was solved to 2.0-Å resolution revealing that the FAD binding and PRODH domain was contained in residues 261–612 [25]. The PRODH domain is a $\beta_8\alpha_8$ barrel with the FAD bound at the C-terminal ends of the beta-strands of the barrel. The PutA669 structure contains the competitive inhibitor L-lactate ($K_i = 1.4$ mM) in the active site providing insights into substrate binding [25,26]. Important ionic bond interactions are formed between the carboxylate group of lactate and Arg555, Arg556, and Lys329. Residues D370 and Y540 form an intimate hydrogen bond pair (distance of 2.7 Å) and are part of a hydrogen bond network that involves R431, K329 and the N(5) atom of FAD. D370 and Y540 also hydrogen bond to the C2 hydroxyl group of lactate and appear to form a ceiling in the active site. A model for proline bound in the active site is illustrated in Fig. 2. The model predicts that several features of the lactate complex will be observed in the proline complex, including the D370–Y540, D370–N368, and Y540–K329 hydrogen bonds, as well as the D370 ion pairs to K329 and R431 (Fig. 2). Neither D370 nor Y540 is expected to hydrogen bond to the proline amine. PutA residues D370 and Y540 are highly conserved in PRODH active sites from other organisms such as human, *Drosophila melanogaster* and *Saccharomyces cerevisiae* [25]. The position of these residues in the PutA669 three-dimensional structure suggests D370 and Y540 may have an important role in proline binding and in determining the redox properties of bound FAD.

In this work, residues D370 and Y540 were investigated by site-directed mutagenesis and tested for their influence

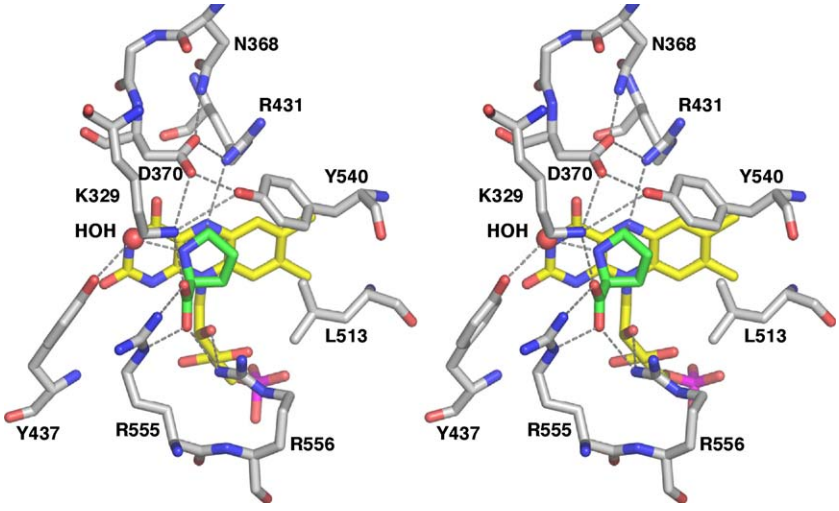

Fig. 2. Stereoscopic view of a model of the substrate proline bound to the PutA86–601 active site. Proline appears in green and FAD in yellow. The dashed lines denote electrostatic interactions. This figure was made with PyMOL. DeLano, W.L. (2002) The PyMOL Molecular Graphics System (http://www.pymol.org).

on steady-state parameters of proline oxidation and FAD redox properties in the PRODH domain of PutA. Because residues 1–86 and 613–669 are missing in the PutA669 structure, a new construct containing residues 86–601 (PutA86–601) was designed to facilitate X-ray structure determination for the PRODH active site mutants. Our aim is to complement site-directed mutagenesis studies of PutA86–601 with three-dimensional structural information to assess conformational rearrangements of active site residues. Here, we report the characterization of mutants D370A, Y540F and D370A/Y540F in PutA86–601 and demonstrate that the D370–Y540 hydrogen bond pair has an important role in shaping proline binding and the midpoint potential (E_m) of FAD in the PRODH domain of PutA.

2. Materials and methods

2.1. Enzymes and chemicals

All chemicals and buffers were purchased from Fisher Scientific and Sigma-Aldrich, Inc. Restriction endonucleases and T4 DNA ligase were purchased from Fermentas and Promega, respectively. Pyocyanine was prepared by photooxidation of phenzine methosulfate. CM-sepharose, Superose-6 material and molecular size standards used for calibrating the size exclusion column were purchased from Sigma. BCA reagents used for protein quantitation were obtained from Pierce. All experiments used Nanopure water.

2.2. Bacterial strains and plasmids

E. coli strains XL-Blue and BL21 DE3 pLysS were purchased from Novagen. The vector pET-23b (Stratagene) containing a hexahistidine encoded sequence was used for expression of PutA86–601 as a C-terminal hexahistidine tagged protein. Sequence-specific synthetic oligonucleotides for site-directed mutagenesis were purchased from Integrated DNA Technologies. The *put* intergenic DNA (419 bp) used for gel shift assays was prepared as described previously using genomic DNA from *E. coli* strain JT31 [23].

2.3. Cloning of wild-type PutA86–601 and site-directed mutants

The PutA86–601 construct (pUTA86–601) was prepared by introducing *Nde*I and *Eco*RI sites in pUTA669 (construct in pET-23b encoding residues 1–669 of PutA with a C-terminal hexahistidine tag) at amino acid codons 84 and 601 by QuikChange site-directed mutagenesis, respectively. Nucleic acid sequencing confirmed the pUT86–601 construct and revealed an Ala541Gly mutation. From the X-ray crystallographic structure of PutA669, however, the mutation is not predicted to affect the properties of PutA86–601. The PRODH active site mutants D370A, Y540F and D370A/Y540F were engineered in pUT86–601 using QuikChange site-directed mutagenesis and confirmed by nucleic acid sequencing. Oligonucleotides used for mutagenesis were 5′-GATATTGGTATCAACATTGCCGCCGAAGAGTCCGATCGC-3′ and 5′-CCGTCCGTGTCGTATTTTTGCTCCGGTTGGCACAC-3′ for D370A and Y540F, respectively.

2.4. Preparation and characterization of PutA86–601

Wild-type PutA86–601 and the mutants D370A, Y540F and D370A/Y540F were overexpressed in *E. coli* strain BL21 DE3 pLysS as described previously for PutA. Pelleted *E. coli* cells were resuspended in 20 mM Tris (pH 7.9) containing 5 mM imidazole, 0.5 M NaCl, 10% glycerol and protease inhibitors phenylmethanesulfonyl fluoride (0.5 mM), L-1-chloro-3-(4-tosylamido)-7-amino-2-heptanone-HCl (0.13 mM), L-1-chloro-3-(4-tosylamido)-4-phenyl-2-butanone (0.08 mM), ε-amino caproic acid (0.08 mM) and leupeptin (1 μM). The resuspended cells were broken by sonication at 4 °C using a pulse sequence of 15 s on and 45 s off (5 min total pulse time). The broken cell debris was removed by centrifugation at 30 000 rpm for 40 min at 4 °C. The cell-free extract was then applied to a Ni^{2+} NTA affinity column (Novagen) and PutA86–601 eluted as previously described for PutA669 [24]. Eluted PutA86–601 was then dialyzed into 50 mM potassium phosphate (pH 7.3) containing 10% glycerol and 2 mM EDTA.

In PutA86–601 the removal of residues 1–85 is predicted to generate an overall basic protein in contrast to the acidic nature of PutA669. The p*I* values for the denatured PutA86–601 and PutA669 polypeptides are calculated to be 8.3 and 6.3, respectively. Since native PutA86–601 is most likely a basic protein, cation exchange chromatography was used for further purification of wild-type PutA86–601 and the mutant proteins. PutA86–601 proteins were applied to a CM-Sepharose column equilibrated with 20 mM potassium phosphate (pH 7.3) containing 10% glycerol and 2 mM EDTA. PutA86–601 proteins were eluted in the same buffer with a gradient of 0–1 M NaCl. During the CM-sepharose column, FAD dissociated from PutA86–601. Activity assays to identify fractions containing PRODH activity were therefore supplemented with FAD. Fractions containing PRODH activity were pooled, incubated with a 10-fold molar excess of FAD and dialyzed overnight at 4 °C in 50 mM potassium phosphate (pH 7.3), 10% glycerol and 2 mM EDTA. After reconstitution of PutA86–601 with FAD, unbound FAD was removed by applying the PutA86–601–FAD mixture to a Bio-Gel P6 column (Bio-Rad) equilibrated with 50 mM potassium phosphate (pH 7.0) containing 10% glycerol and 2 mM EDTA. Wild-type PutA86–601 and mutant proteins were then concentrated using an Amicon ultrafiltration cell with a 30-kDa molecular-weight cutoff, frozen in liquid nitrogen, and stored at −70 °C. The C-terminal hexahistidine tag was retained after purification of each protein. Thus, all PutA86–601 proteins

contained a fusion hexahistidine tag at the C-terminal in the experiments. The homogeneity of the final purified PutA86–601 proteins was estimated by SDS-PAGE analysis to be >95%.

The concentrations of the purified PutA86–601 enzymes were determined by the BCA method and spectrophotometrically using the estimated molar extinction coefficients for each enzyme at the main FAD absorbance band (see Table 1). The molar extinction coefficients were estimated as previously described by denaturing each PutA86–601 protein in 6 M guanidinium chloride and quantitating the amount of released FAD using the molar extinction coefficient of 11.8 mM^{-1} cm^{-1} at 445 nm for free FAD [24]. The reported molar extinction coefficients for wild-type PutA86–601 and the site-directed mutants are the average values from two independent determinations and have standard deviations of $\pm$ 0.2–0.4 mM^{-1} cm^{-1}. The molar ratio of FAD to wild-type PutA86–601 and the mutant polypeptides was assessed by comparing the total amount of denatured polypeptide to the total amount of released FAD as described previously [24]. The molecular mass of wild-type PutA86–601 was estimated by size exclusion chromatography on a Superose 6 column at 4 °C that had been calibrated using the molecular mass standards carbonic anhydrase (29 kDa), bovine serum albumin (66 kDa), alcohol dehydrogenase (150 kDa), β-amylase (200 kDa), and apoferritin (443 kDa). The DNA binding activity of wild-type PutA86–601 was tested by nondenaturing gel mobility shift assays as described for PutA669 using 0–2 μM PutA86–601 and 20 nM *put* control intergenic DNA in the binding reactions [24].

2.5. Steady-state kinetics

The Michaelis–Menten parameters (K_m and V_{max}) for PRODH activity of wild-type PutA86–601 and mutants D370A, Y540F and D370A/Y540F were determined in 100 mM MOPS buffer (pH 8.0) at 25 °C by varying proline concentration. PRODH activity was measured using dichlorophenolindophenol (DCPIP) as a terminal electron acceptor and phenazine methosulfate as a mediator (Proline: DCPIP oxidoreductase assay) as previously described [23]. One unit of PRODH activity is the quantity of enzyme, which transfers electrons from 1 μmol of proline to DCPIP per minute at 25 °C. Assays were initiated by adding enzyme and were performed in triplicate. The kinetic parameters K_m and k_{cat} were estimated by nonlinear regression to the Michaelis–Menten equation and by Lineweaver–Burk plot analysis of the initial reaction velocity vs. proline concentration [27]. To determine the K_m and k_{cat} parameters of wild-type PutA86–601, D370A, Y540F and D370A/Y540F for FAD, proline:DCPIP oxidoreductase assays were performed with wild-type PutA86–601 and mutant apoproteins in 100 mM MOPS buffer (pH 8.0) at 25 °C with varying FAD concentrations (0–3 μM). PutA86–601 apoproteins were obtained directly from the CM-sepharose column. From the UV–visible spectra of the PutA86–601 apoproteins, the amount of residual FAD remaining in each apoprotein preparation was estimated at < 1%.

Table 1
Spectroscopic properties[a] and midpoint potentials for wild-type and mutant PutA86–601

Enzyme	λ_{max} (nm)		ε_λ (mM^{-1} cm^{-1})		E_m (mV)
	1	2	1	2	
Wild-type	379	451	10.6	13.9	− 66 ± 3
D370A	379	450	13.0	13.9	− 26 ± 4
Y540F	381	450	12.5	13.3	− 89 ± 3
Y540F/D370A	380	450	12.0	13.2	− 42 ± 2

[a] Maximum wavelength (λ_{max}) and corresponding molar extinction coefficient (ε_λ) at pH 7.0.

The effect of pH on the kinetic parameters of wild-type PutA86–601 and mutants D370A, Y540F and D370A/Y540F for proline was determined at 25 °C from pH 6.0 to 10.0 using a mixed buffer system comprised of 20 mM each MES, MOPS, HEPES, TABS and CHES. Assays were performed in triplicate and values for K_m and k_{cat} were estimated by nonlinear regression to the Michaelis–Menten equation. Inhibition of PRODH activity in wild-type PutA86–601 and D370A/Y540F by L-tetrahydro-2-furoic acid (L-THFA) was measured from pH 6.0 to 9.0 at 25 °C using the mixed buffer system described above. Assays were performed in triplicate and the apparent inhibition constants (K_i) for wild-type PutA86–601 and D370A/Y540F were determined by Dixon plots of 1/velocity vs. L-THFA concentration (0–2 mM) as previously described [26,28]. The stability of wild-type PutA86–601 and mutants D370A, Y540F and D370A/Y540F at different pH values was tested by incubating the PutA86–601 proteins in the mixed buffer at pH 6.0–10.0 for 2 h. PRODH activity assays were then performed for each protein sample at pH 8.0 to assess PutA86–601 stability in pH 6.0–10.0.

The pH profiles of the kinetic parameters for wild-type PutA86–601 and mutants D370A, Y540F and D370A/Y540F were analyzed according to Dixon [29] and Cleland [30] for the effect of pH on enzyme–ligand complexes by plotting log k_{cat}, log k_{cat}/K_m, pK_m, and pK_i vs. pH. The associated pK_a values for the effect of pH on the kinetic parameters were determined by best-fit analysis to Eqs. (1) and (2) using Sigma Plot 8.0 Enzyme Kinetics where P_{obs} and P_{lim} represent the observed and limiting parameter values, respectively, and pK_a is the acid

$$P_{obs} = P_{lim}/(1 + 10^{\wedge(pK_a - pH)}) \quad (1)$$

$$P_{obs} = (P_{lim1} + P_{lim2} * 10^{\wedge(pH - pK_a)})/(1 + 10^{\wedge(pH - pK_a)}) \quad (2)$$

dissociation constant of an ionizable group in the pH range studied. Eq. (1), which describes an increase in activity upon deprotonation of a group, was used for analyzing the effect of pH on k_{cat} for each PutA86–601 protein and k_{cat}/K_m for

wild-type PutA86–601 and mutants D370A and Y540F. Eq. (2), which estimates limiting parameter values at low and high pH, was used to analyze the pH profile of k_{cat}/K_m for PutA86–601 mutant D370A/Y540F. The associated pK_a values for the effect of pH on K_m and K_i for wild-type PutA86–601 and mutant D370A/Y540F were also estimated using Eq. (2). As described by Dixon [29], in plots of pK_m and pK_i vs. pH, downward curvature indicates ionization of free enzyme or substrate while upward curvature indicates an ionization event on the enzyme–substrate (E–S) complex.

2.6. Spectroelectrochemistry

Potentiometric and coulometric measurements of wild-type PutA86–601 and mutants D370A, Y540F, and D370A/Y540F were performed as previously described under an argon atmosphere using a three-electrode single compartment spectroelectrochemical cell containing a gold wire working electrode, a silver/silver chloride reference electrode, and a silver wire counter electrode [23,31]. All potential values are reported relative to the normal hydrogen electrode and were determined in the reductive direction. Potentiometric measurements were recorded at 23 °C in 50 mM potassium phosphate (pH 7.0), 10% glycerol, and 2 mM EDTA. Methyl viologen (0.1 mM) and potassium ferrocyanide (0.1 mM) were used as mediator dyes and pyocyanine ($E_m = -0.04$ V, pH 7.5) (5 μM) and indigo disulfonate ($E_m = -0.109$ V, pH 7.5) (2–5 μM) were used as indicator dyes [23]. PutA86–601 concentrations were typically between 20 and 25 μM in the potentiometric experiments. Equilibration of the system in the potentiometric experiments was considered to be obtained when the measured potential change was less than 1 mV in 5 min; this was typically 1–2 h. The UV–visible spectra in each experiment were recorded from 300–800 nm on a Cary 100 spectrophotometer. The absorbance at 451 nm was used to monitor the amount of oxidized and reduced FAD. Clean spectra of PutA86–601 in the potentiometric experiments were obtained by subtracting the spectra of the mediator and indicator dyes in the absence of protein which were measured under identical conditions. Occasionally the spectra were also corrected for turbidity based on the increases in the absorbance at 800 nm during the potentiometric titration. To ensure the system was reversible and at equilibrium, the solution was periodically reoxidized during the potentiometric experiments by switching the applied potential from −0.8 to +0.8 V. The midpoint potentials (E_m) and n values were calculated from the Nernst equation (Eq. 3) where E is the measured equilibrium potential at each point in the titration and n is the number of electrons

$$E = E_m + (0.059/n)\log[(ox)/(red)] \quad (3)$$

transferred. Nernst plots of the potentiometric measurements for wild-type PutA86–601 and mutants D370A, Y540F and D370A/Y540F all generated slopes near the theoretical value of 28 mV for a $2e^-$ transfer. Titrations of wild-type PutA86–601 and the mutant D370A with proline were performed at 25 °C in 50 mM potassium phosphate buffer (pH 7.0) containing 10% glycerol under anaerobic conditions and the data were analyzed as previously described [23].

3. Results

3.1. PutA86–601 properties

The predicted molecular weight of the PutA86–601 polypeptide is 59557 Da. A molecular mass of 52.5 kDa for wild-type PutA86–601 was estimated by size exclusion chromatography indicating PutA86–601 purifies as a monomer. This is in contrast to PutA669 which previously was shown to purify as a dimer [24,25]. In addition to loss of dimerization, PutA86–601 does not bind the *put* control DNA region even with 100-fold excess of PutA86–601 relative to DNA in the binding reaction. Thus, it appears that deletion of the N-terminal region removes the oligomeric and DNA-binding properties of PutA669 and generates a monofunctional PRODH enzyme. The UV–visible spectral data for wild-type PutA86–601 and PutA86–601 mutants D370A, Y540F and D370A/Y540F are summarized in Table 1. The UV–visible spectrum of wild-type PutA86–601 exhibits two absorption maxima at 451 and 379 with a 451/379 ratio of 1.19 that is higher than the 451/381 ratio of PutA (1.05) and PutA669 (1.09) (see Fig. 5) [23,24]. The amount of bound FAD was consistently about 0.8–0.85 mol of FAD per mole of polypeptide for wild-type PutA86–601. No significant changes in the UV–visible spectra of the PutA86–601 mutants D370A, Y540F and D370A/Y540F were observed relative to wild-type PutA86–601 except for generally lower FAD amounts of around 0.65–0.7 mol of FAD per mol of polypeptide. The molar extinction coefficients of the main FAD absorption band for wild-type PutA86–601 and mutants D370A, Y540F and D370A/Y540F ranged from 13.2 to 13.9 mM^{-1} cm^{-1} (Table 1). Incubation of wild-type PutA86–601 and mutants D370A, Y540F and D370A/Y540F at various pH values showed no significant decrease in PRODH activity, indicating that the PutA86–601 proteins were fairly stable between pH 6.0 and 10.0 for 2 h.

3.2. Steady-state kinetics

The K_m, k_{cat}, and K_m/k_{cat} values for L-proline determined at pH 8.0 for wild-type PutA86–601 and mutants D370A, Y540F and D370A/Y540F are summarized in Table 2. The kinetic parameters of wild-type PutA86–601 for proline are slightly improved from the previously determined K_m and k_{cat} values for PutA of 100 mM and 7.6 s^{-1}, respectively [23]. The k_{cat} value of wild-type PutA86–601 is similar to the turnover number for

Table 2
Kinetic constants for PRODH activity in PutA86–601[a]

Enzyme	K_m (mM)	k_{cat} (s^{-1})	k_{cat}/K_m (s^{-1} M^{-1})
Wild type	58 ± 5	20 ± 0.6	345
D370A	73 ± 7	9.7 ± 0.3	124
Y540F	300 ± 25	1.8 ± 0.7	60
Y540F/D370A	340 ± 30	7.8 ± 0.6	23

[a] Parameters were estimated by best-fit analysis to the Michaelis–Menten equation.

PutA669 (19 s^{-1}) [24]. In the D370A mutant the K_m for proline is comparable to wild-type PutA86–601 but the k_{cat} value is about twofold lower. A fivefold increase in K_m relative to wild-type PutA86–601 was observed with the Y540F mutant while k_{cat} remained similar. For the D370A/Y540F mutant, almost a sixfold increase in K_m for proline and about a twofold decrease in k_{cat} relative to wild-type PutA86–601 were determined. The most significant change in k_{cat}/K_m was observed for D370A/Y540F with a value about 15-fold lower than wild-type PutA86–601. Evaluation of the kinetic parameters of wild-type PutA86–601 and mutant apoproteins for FAD showed similar trends in the kinetic parameters (data not shown). A K_m of 0.2 μM for FAD and a k_{cat} value of 8 s^{-1} were estimated for wild-type PutA86–601 apoprotein. Apoproteins D370A and Y540F have similar k_{cat} values relative to wild-type PutA86–601 and K_m values of 0.4 μM for FAD. The mutant D370A/Y540F exhibited the largest change in kinetic parameters with a threefold increase in K_m for FAD (0.6 μM) and a fourfold decrease in k_{cat} (2.3 s^{-1}) relative to wild-type PutA86–601. Thus, the elimination of the D370–Y540 hydrogen bond pair in the D370A/Y540F mutant affects proline and FAD binding and slightly diminishes k_{cat} resulting in noticeably lower k_{cat}/K_m values for proline and FAD relative to wild-type PutA86–601.

To further probe the role of D370A and Y540F in the PRODH reductive half-reaction, a pH profile was determined for the kinetic parameters k_{cat} and k_{cat}/K_m for wild-type PutA86–601 and the mutants D370A, Y540F, and D370A/Y540F. In Fig. 3, plots of log k_{cat} and log k_{cat}/K_m vs. pH for each PutA86–601 protein are shown in the upper and lower panels, respectively. The k_{cat} and k_{cat}/K_m parameters reach plateaus at high pH for wild-type PutA86–601 and each mutant. In the mutant D370A/Y504F a plateau for k_{cat}/K_m also seems to emerge at low pH. Estimated pK_a values for the pH-dependent increase in k_{cat} range from 6.4 to 7.0 with a pK_a value of 6.9 for wild-type PutA86–601 (Fig. 3, top). Fig. 3 (top) illustrates that deprotonation of a group on the E–S complex is important for catalysis and occurs at similar pH values in wild-type PutA86–601 and the PutA86–601 mutants. The pH dependence of k_{cat}/K_m is more varied, namely between wild-type PutA86–601 (pK_a = 6.9) and the mutant D370A/Y540F (pK_a = 8.4). Apparently, an ionization event that affects proline binding and catalysis occurs in D370/Y540F that is not observed in wild-type PutA86–601. Since the effect of pH on k_{cat} is similar for wild-type PutA86–601 and the mutants, the $\Delta pK_a \sim 1.5$ between wild-type PutA86–601 and D370A/Y540F for the pH dependence of k_{cat}/K_m appears to be due to an ionization that affects proline binding. Fig. 4 shows the pH dependence of K_m for proline in wild-type PutA86–601 and D370A/Y540F. A plot of pK_m vs. pH for wild-type PutA86–601 revealed that the K_m for proline is pH independent from pH 7.0 to 10.0 (Fig. 4). In contrast, a plot of pK_m vs. pH for D370A/Y540F demonstrated a sixfold decrease in the K_m for proline for which a pK_a value of 8.2 was estimated (Fig. 4). The upward curvature of the pK_m vs. pH plot for D370A/Y540F indicates ionization of a group on the E–S complex. The effect of pH on K_m was also evaluated for D370A and

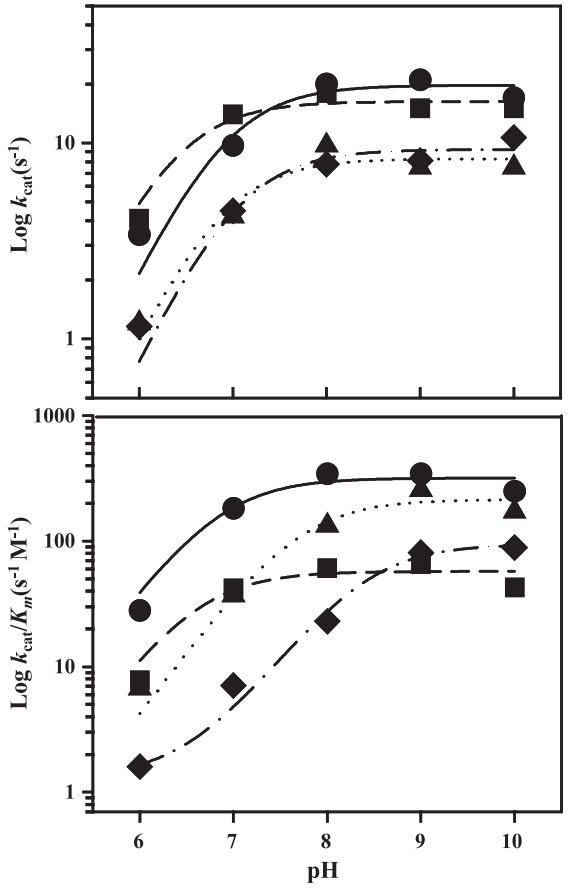

Fig. 3. Kinetic pH profiles of parameters k_{cat} and k_{cat}/K_m for PutA86–601. Measurements were performed in a 100 mM mixed buffer from pH 6.0 to 10.0 at 25 °C. (Top) Plot of log k_{cat} vs. pH for wild-type (●), D370A (▲), Y540F (■), and D370A/Y540F (♦). Data were fit to Eq. (1) for wild-type (—), D370A (···), Y540F (– –), and D370A/Y540F (–·–) PutA86–601 to yield pK_a values of 6.9 ± 0.2, 6.9 ± 0.3, 6.4 ± 0.2 and 7.0 ± 0.2, respectively, for the pH-dependent increase in k_{cat}. (Bottom) Plot of log k_{cat}/K_m vs. pH for wild-type (●), D370A (▲), Y540F (■), and D370A/Y540F (♦). Fits to the data were performed for wild-type (—), D370A (···) and Y540F (– –) PutA86–601 using Eq. (1) and D370A/Y540F (–·–) PutA86–601 using Eq. (2). The pK_a values estimated from the fits were 6.9 ± 0.3, 7.7 ± 0.3, 6.6 ± 0.3 and 8.4 ± 0.1 for wild-type, D370A, Y540F and D370A/Y540F PutA86–601, respectively.

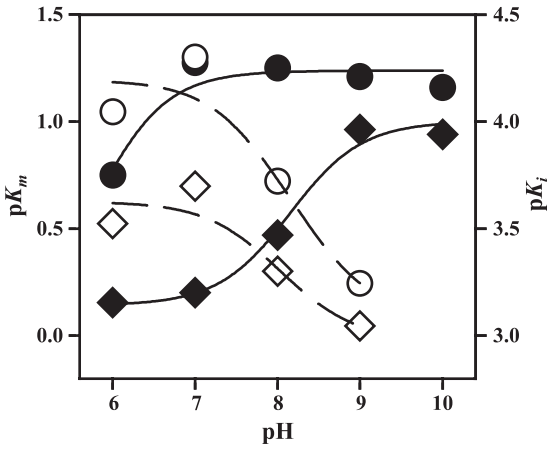

Fig. 4. Kinetic pH profiles of parameters K_m for proline and K_i for L-THFA with wild-type and D370A/Y540F PutA86–601 at 25 °C. The effect of pH on K_m (solid symbols) and K_i (open symbols) for wild-type (circles) and D370A/Y540F (diamonds) PutA86–601 was analyzed by plotting pK_m and pKi vs. pH. Best-fit analysis of the data using Eq. (2) is shown for pK_m vs. pH (solid curves) and pK_i vs. pH (dashed curves). The pK_a values estimated from the fits are 8.2 ± 0.2 for the pH-dependent decrease in K_m observed for D370A/Y540F and 8.7 ± 0.3 and 8.4 ± 0.4 for the pH-dependent increase observed in K_i for wild-type and D370A/Y540F PutA86–601, respectively.

Y540F and showed overall decreases in K_m of threefold and twofold from pH 7.0 to 10.0, respectively, but reasonable estimates of associated pK_a values could not be obtained (data not shown). Thus, the variation in pH dependence of log k_{cat}/K_m of wild-type PutA86–601 and D370A/Y540F is caused by dissimilar pH-dependent changes in apparent proline binding affinity.

Interpretation of the pH-dependent proline binding affinity of D370A/Y540F was attempted by comparing the pH dependence of K_m for proline and the inhibition constant (K_i) for L-THFA. L-THFA is a competitive inhibitor of PRODH activity in PutA with a $K_i = 0.2$ mM at pH 8.0 (or $K_d = 0.24$ mM, pH 8.0) [26]. Unlike proline, L-THFA does not have an ionizable group in the pH range under study (see Fig. 1). Fig. 4 shows plots of pK_i vs. pH for the inhibition of wild-type PutA86–601 and D370A/Y540F by L-THFA. At pH 8.0, a 2.5-fold difference in K_i for L-THFA was observed between wild-type PutA86–601 ($K_i = 0.2$ mM) and D370A/Y540F ($K_i = 0.5$ mM). This is smaller than the disparity observed in K_m for proline between wild-type PutA86–601 and D370A/Y540F at pH 8.0. The pH dependence of K_i for L-THFA in wild-type PutA86–601 and D370A/Y540F is similar with increases from 0.09 (pH 6.0) to 0.6 mM (pH 9.0) for wild-type PutA86–601 and 0.3 (pH 6.0) to 0.9 mM (pH 9.0) for D370A/Y540F. The observed pH-dependent increases of K_i in wild-type PutA86–601 and mutant D370A/Y540F are characterized by pK_a values of about 8.7 and 8.4, respectively. The downward curvature of the pK_i vs. pH plots indicates an ionization event on the free enzyme or substrate. Since L-THFA does not have an ionizable group in the pH range studied, the pK_a associated with the pH dependence of K_i must be a group on the enzyme. On the basis of the proline binding model, an ionizable group in the active site that might influence L-THFA binding is the hydroxyl group of Y437 (Fig. 2). Another suitable candidate is K329. Because the pH profiles of K_m and K_i for the D370A/Y540F mutant are clearly different, the effect of pH on the apparent proline binding affinity in D370A/Y540F appears to be due to ionization of the secondary amine group of proline in the E–S complex. The p$K_a \sim 8.2$ for the pH dependence of K_m for proline in D370A/Y540F therefore represents the ionization of the proline amine in the E–S complex, which is shifted from the p$K_a \sim 10.5$ for free proline.

3.3. Spectroelectrochemistry

Wild-type PutA86–601 and the mutants D370A, Y540F and D370A/Y540F were characterized by spectroelectrochemistry to assess the impact of these residues on the FAD redox and PRODH active site environment. Fig. 5 shows a coulometric titration of wild-type PutA86–601. Two electron equivalents were required to fully reduce the FAD bound to wild-type PutA86–601. Red anionic semiquinone was observed at about 1 equiv of electrons ($n = 1$) with maximum absorbance occurring at 371 nm. The molar absorptivities for the fully reduced enzyme were calculated to be 997 and 4752 M^{-1} cm^{-1} at 451 and 371 nm, respec-

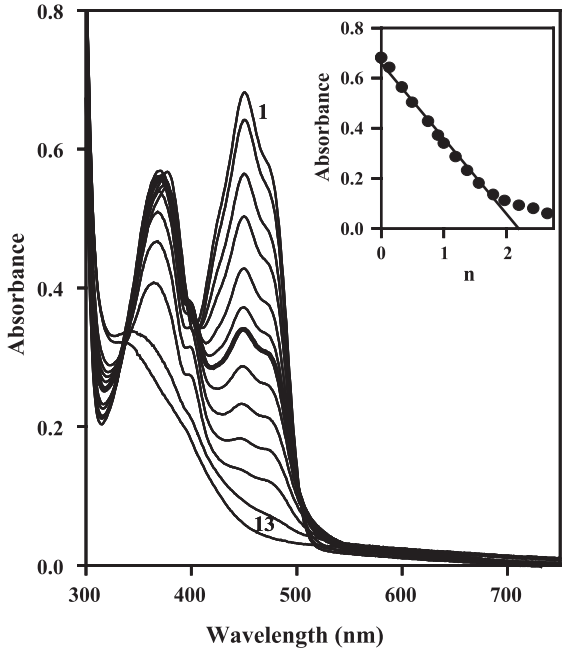

Fig. 5. Coulometric titration of wild-type PutA86–601 (49.2 μM) with 100 μM methyl viologen at 25 °C in 50 mM potassium phosphate buffer (pH 7.0) containing 10% glycerol and 2 mM EDTA. Curves 1–12; $n = 0$, 0.13, 0.33, 0.49, 0.75, 0.9, 1.0, 1.18, 1.37, 1.56, 1.78, and 2.2, respectively. Curve 13, fully reduced spectrum. Curve 6 ($n = 1.0$) is in bold to highlight the spectrum of wild-type PutA86–601 at half-reduction showing maximum formation of the red anionic semiquinone. The inset shows the plot of absorbance at 451 nm vs. the number of reducing equivalents.

tively. Using the previously determined molar absorptivities of 15450 M^{-1} cm^{-1} at 371 nm and 3540 M^{-1} cm^{-1} at 451 nm for the red anionic semiquinone in PutA, the maximum amount of semiquinone stabilized during electrochemical reduction of wild-type PutA86–601 was estimated to be about 30%, slightly higher than that previously observed for PutA and PutA669 [23]. Coulometric titrations of the mutants D370A (Fig. 6) and Y540F were also performed and confirmed that two electron equivalents were required for complete reduction of the bound FAD. The maximum amount of red anionic semiquinone stabilized during the coulometric titrations was estimated at 20–25% for D370A and <10% for Y540F.

Next, potentiometric titrations were performed to assess the influence of D370 and Y540 on the midpoint potential (E_m) of bound FAD. The potentiometric data for each of the PutA86–601 proteins are summarized in Table 1. An E_m value of −66 mV (pH 7.0) for wild-type PutA86–601 was determined and is about 10 mV more positive than that reported earlier for the dimeric form of the PRODH domain, PutA669 (E_m = −76 mV, pH 7.0) [24]. A 40-mV positive shift in the midpoint potential of D370A (E_m = −26 mV, pH 7.0) relative to wild-type PutA86–601 was determined with a Nernst slope of 37 mV (Fig. 6, inset). This corresponds to a Gibbs free energy difference of ~ −1.8 kcal mol^{-1} and indicates a tighter binding affinity of reduced FAD to D370A

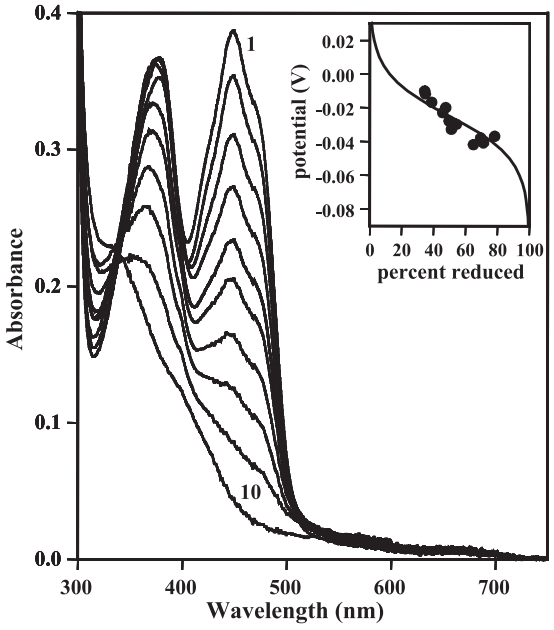

Fig. 6. Coulometric titration of D370A PutA86–601 (27.8 μM) with 100 μM methyl viologen at 25 °C in 50 mM potassium phosphate buffer (pH 7.0) containing 10% glycerol and 2 mM EDTA. Curves 1–9; n = 0, 0.25, 0.53, 0.77, 1.03, 1.31, 1.60, 1.90, and 2.2, respectively. Curve 10, fully reduced spectrum. Curve 5 (n = 1.03) is in bold to highlight the spectrum of D370A PutA86–601 at half-reduction. The inset shows a fit of the reduction potential data for D370A PutA86–601 (pH 7.0) to a theoretical curve generated from the Nernst equation for one redox center with E_m = −0.026 V (n = 2).

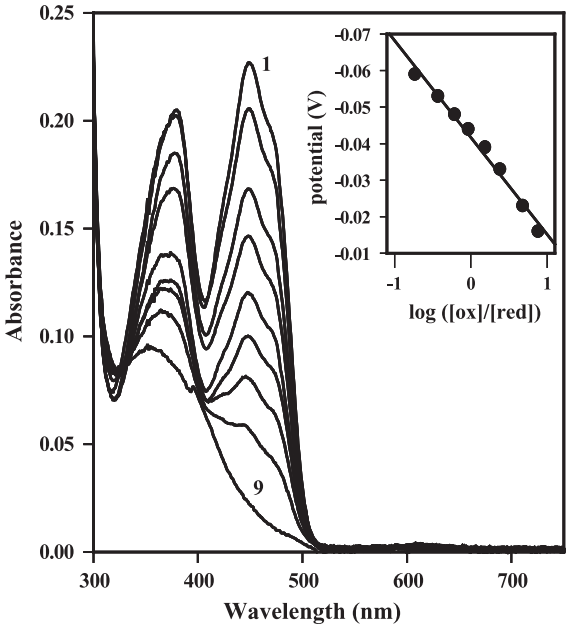

Fig. 7. Potentiometric titration of D370A/Y540F PutA86–601 (17. 2 μM). Titration was performed in 50 mM potassium phosphate buffer (pH 7.0) at 25 °C (curves 1–9; fully oxidized, −0.016, −0.033, −0.039, −0.044, −0.048, −0.053, −0.059 V, and fully reduced, respectively). The inset is a Nernst plot of the potentiometric data for D370A/Y540F indicating E_m = −0.042 V with a 27-mV slope.

relative to wild-type PutA86–601. Even though D370A has a more positive E_m value relative to wild-type PutA86–601, proline reduction of bound FAD in D370A is slightly less favorable. The equilibrium constants for proline reduction of D370A and wild-type PutA86–601 are 31 and 52 mM^{-1} proline, respectively, equivalent to a Gibbs free energy difference of ~ 1.3 kcal mol^{-1}. Potentiometric titrations of Y540F yielded an E_m value of −89 mV (pH 7.0) with a Nernst slope of 32 mV (data not shown) resulting in a 23-mV shift in the negative direction relative to wild-type PutA86–601. A midpoint potential of −42 mV (pH 7.0) with a Nernst slope of 27 mV was determined for D370A/Y540F (Fig. 7). Thus, the D370A mutation causes the E_m to shift positive by 40 mV relative to wild-type PutA86–601 and 47 mV relative to Y540F. The 47-mV positive shift in the midpoint potential observed for the D370A/Y540F mutant relative to the Y540F mutant translates into a Gibbs free energy difference of ~ −2.2 kcal mol^{-1}.

4. Discussion

Site-directed mutagenesis studies of the PRODH active site were initiated using PutA86–601 to mimic the known structural form of PutA (PutA87–612) [25]. The catalytic and spectroelectrochemical properties of wild-type PutA86–601 are similar to PutA669 showing that the FAD binding environment has not changed upon removal of the N-terminal domain [24]. From the X-ray

crystal structure of PutA669, D370 and Y540 participate in an extensive hydrogen bond and ion pair network in the PRODH active site. The importance of these residues is underscored by their conservation among PRODH enzymes from various organisms. In our study the apparent binding affinity for oxidized FAD and the UV-spectra of bound FAD were similar for wild-type PutA86–601 and the mutants D370A, Y540F, and D370A/Y540F. Thus, the mutations do not appear to cause any significant changes in the overall conformation of the FAD binding site and PRODH domain. It is anticipated that X-ray crystallographic data on the PutA86–601 mutants will be obtained to understand the structural impact of each mutation.

Disruption of the D370–Y540 hydrogen bond pair generates various changes in steady-state kinetic parameters of the PRODH reductive-half reaction. The small changes in k_{cat} and similar pH dependence for k_{cat} indicate that residues D370 and Y540 are not critical for deprotonation of proline in the reductive half-reaction (see Fig. 1). This result agrees with the proposed structural model (Fig. 2), in which neither residue is within hydrogen bonding distance of the proline N atom. Y437 and an active site water molecule observed in the X-ray crystal structure of the PutA669–lactate complex (Fig. 2) are more likely to have a role in a proton abstraction step [25]. From the proline binding model, the C(5) atom of proline is 3.2 Å from the N(5) position of FAD indicating that a hydride transfer step is feasible for the proline reductive half-reaction. Also, PutA reconstituted with 5-deazaFAD, a nicotinamide-type flavin analogue, can be reduced by proline showing that hydrogen transfer from the C(5) of proline to FAD is at least operable in PutA [32,33]. Reactions analogous to PRODH are catalyzed by the flavin-dependent amino acid and monoamine oxidases. Strong evidence supports a concerted hydride transfer mechanism in D-amino acid oxidase for the oxidation of D-amino acids to imino acids [34,35]. In monoamine oxidases, however, amine oxidation has been suggested to occur by single electron transfer steps to the flavin or by a concerted mechanism involving a covalent intermediate with the flavin [36]. Future mechanistic studies will aim at resolving whether proline oxidation in PRODH occurs by a hydride transfer mechanism.

Removal of both hydrogen bonding partners in the PutA86–601 mutant D370A/Y540F decreases the turnover number and apparent proline binding affinity to yield an overall catalytic efficiency that is 15-fold lower than wild-type PutA86–601. Significant differences between wild-type PutA86–601 and D370A/Y540F were also evident in the pH profiles of k_{cat}/K_m ($\Delta pK_a \sim 1.5$) and K_m for proline. The apparent proline binding affinity is relatively pH independent in wild-type PutA86–601 while in D370A/Y540F a decrease in K_m for proline is observed with an estimated $pK_a \sim 8.2$. Dixon analysis of the pH effect on K_m in the PutA86–601 mutant D370A/Y540F showed an upward curvature indicating ionization of the E–S complex. Since only electrostatic interactions are lost with D370A or Y540F, we considered that the D370–Y540 hydrogen bond pair may have a role in countering the positively charged secondary amine group of proline in the E–S complex. To assess whether the observed pK_a for the ionizable group on the E–S complex is due to the secondary amine group of proline, the pH profile of PRODH inhibition by L-THFA was measured for wild-type and the D370A/Y540F mutant. Unlike the pH profiles of K_m for proline, wild-type PutA86–601 and D370A/Y540F exhibit a similar pattern of a pH-dependent increase in K_i for L-THFA. The contrasting pH dependence of K_m for proline and K_i for L-THFA in D370A/Y540F indicates that the pH dependence of K_m in D370A/Y540F is related to ionization of proline in the E–S complex. In wild-type PutA86–601 the D370–Y540 pair may provide interactions that help accommodate a $-NH_2^+-$ moiety in the active site at $pH < pK_a$ of the secondary amine group of proline in the E–S complex. D370A/Y540F lacks these ionic interactions resulting in a higher K_m value for the zwitterionic form of proline ($-NH_2^+-$) at pH < 8.2. Conversely, at pH>8.2 proline is expected to be in the anionic form (–NH–) in the E–S complex resulting in more favorable proline binding as evident by a K_m value of about 100 mM proline for D370A/Y540F at pH 10.0.

Interestingly, deletion of the carboxylate group of D370 and the hydroxyl group of Y540F had opposite effects on the midpoint potential of the bound FAD. The measured midpoint potential for bound FAD shifted in the positive direction ($\Delta E_m \sim 40$ mV) for D370A and slightly in the negative direction ($\Delta E_m \sim -23$ mV) for Y540F relative to wild-type PutA86–601. Similar to D370A, the E_m of FAD bound to D370A/Y540F (-42 mV, pH 7.0) was also more positive than the E_m for wild-type PutA86–601. Disruption of the D370–Y540 hydrogen bond pair most likely causes new orientations of D370 and its hydrogen bond partners. Reduction of FAD increases electron density across the N(1), C(4a), and N(5) positions of the isoalloxazine ring. Increased flexibility of D370 in the active site of the Y540F mutant may allow the acidic residue to move closer to the C(4a) and N(5) moieties making reduction of FAD more difficult. Electrostatic effects on flavin reduction potentials have been studied extensively for flavodoxin in which a strong correlation between the number of acidic residues around the flavin and the reduction potential of the semiquinone/hydroquinone couple was demonstrated [37]. Alternatively, D370 may interact more strongly with R431 in the Y540F mutant. The NH1 atom of R431 is 2.9 Å from the FAD N(5) atom in the X-ray crystal structure of the PutA669–lactate complex [25]. A stronger ion pair between D370 and R431 could alter the conformation of R431 and partly undermine its stabilizing influence on FAD reduction causing a slightly lower E_m for the Y540F mutant. Charged groups, such as the Arg guanidinium, that are near the flavin have been shown to influence reduction potentials in flavoproteins [38,39]. In the electron-transferring flavoprotein (ETF) from *Methylophilus methylotrophus*, the reduction potential for the oxidized/semiquinone couple shifted about

200 mV lower upon replacing Arg237 with Ala in the active site establishing that Arg237 has a major role in stabilizing the anionic semiquinone of FAD in ETF [39]. In D370A and D370A/Y540F, not only is the D370–Y540 hydrogen bond pair disrupted as in Y540F but also D370–R431 interactions allowing R431 to explore other conformations. As a result, the D370A mutation not only removes a negatively charged carboxylate group from the FAD binding site but most likely induces rearrangements of R431 in the active site that stabilize the reduced form of FAD and raise the E_m of bound FAD. Therefore, the divergent affects on the FAD redox properties in D370A and Y540F may be mediated by subtle changes in the proximity of R431 to the N(5), C(4a), and N(1) positions of FAD. The importance of R431 in FAD binding was evident in attempts to purify the PutA86–601 mutant R431A which could only be reconstituted with <0.1 mol of FAD per mole of R431 polypeptide (data not shown). Future work will focus on characterizing the influence of R431 on FAD redox properties and PRODH activity in PutA.

During the design and characterization of PutA86–601, it became apparent that deletion of N-terminal residues 1–85 disrupts the dimeric structure and DNA-binding activity of PutA669. From the X-ray crystallographic structure, a dimerization domain was hypothesized to include residues 87–139 which interact with the $\beta_8\alpha_8$ barrel of the PRODH domain [25]. It is surprising that PutA86–601 purifies as a monomer since it retains the previously postulated dimerization domain. Thus, dimerization most likely involves residues not observed in the three-dimensional structure and emphasizes that the dimerization of PutA is not yet clearly defined. Likewise, the lack of DNA-binding also points to a different model than that described from the PutA669 structure. Clearly, more work is needed to clarify the role that the N-terminal domain has on PutA functions. Nevertheless, the successful isolation of PutA86–601 shows that dimerization is not necessary for forming a stable and active PRODH domain. Investigations are underway to define the role that the N-terminal region has on PutA functions. For example, PutAΔ85 was recently shown to be a monomer confirming that the N-terminal 1–85 residues are important for dimerization of the PutA protein and might be critical for the functional versatility of PutA (Baban, B.A. and Becker, D.F., unpublished data).

Acknowledgements

This research was supported in part by the Research (Award RI0384), ACS-PRF (36470-G4), NSF (MCB0091664), NIH grants GM61068 (Becker) and GM65546 (Tanner), University of Nebraska Biochemistry Department and Redox Biology Center, and the Nebraska Agricultural Research Division, Journal Series No. 14474. This publication was also made possible by NIH Grant Number P20 RR-017675-02 from the National Center for Research Resources. Its contents are solely the responsibility of the authors and do not necessarily represent the official views of the NIH.

References

[1] S.A. Maxwell, G.E. Davis, Differential gene expression in p53-mediated apoptosis-resistant vs. apoptosis-sensitive tumor cell lines, Proc. Natl. Acad. Sci. U. S. A. 97 (2000) 13009–13014.
[2] S.P. Donald, X.Y. Sun, C.A. Hu, J. Yu, J.M. Mei, D. Valle, J.M. Phang, Proline oxidase, encoded by p53-induced gene-6, catalyzes the generation of proline-dependent reactive oxygen species, Cancer Res. 61 (2001) 1810–1815.
[3] C.H. Hagedorn, J.M. Phang, Catalytic transfer of hydride ions from NADPH to oxygen by the interconversion of proline to Δ^1-pyrroline-5-carboxylate, Arch. Biochem. Biophys. 248 (1986) 166–174.
[4] S. Vílchez, L. Molina, C. Ramos, J.L. Ramos, Proline catabolism by *Pseudomonas putida*: cloning, characterization, and expression of the *put* genes in the presence of root exudates, J. Bacteriol. 182 (2000) 91–99.
[5] D.E. Culham, J. Henderson, R.A. Crane, J.M. Wood, Osmosensor ProP of *Escherichia coli* responds to the concentration, chemistry, and molecular size of osmolytes in the proteoliposome lumen, Biochemistry 42 (2003) 410–420.
[6] J.M. Wood, Proline porters effect the utilization of proline as a nutrient of osmoprotectant for bacteria, J. Membr. Biol. 106 (1988) 183–202.
[7] J.M. Phang, The regulatory functions of proline and Δ^1-pyrroline-5-carboxylic acid, Curr. Top. Cell. Regul. 25 (1985) 92–132.
[8] J.L.A. Abrahamson, L.G. Baker, J.T. Stephenson, J.M. Wood, Proline dehydrogenase from Escherichia K12, properties of the membrane-associated enzyme, Eur. J. Biochem. 134 (1983) 77–82.
[9] E. Brown, J.M. Wood, Redesigned purification yields a fully functional PutA protein dimer from *Escherichia coli*, J. Biol. Chem. 267 (1992) 13086–13092.
[10] R. Menzel, J. Roth, Enzymatic properties of the purified *putA* protein from *Salmonella typhimurium*, J. Biol. Chem. 256 (1981) 9762–9766.
[11] M.L. Efron, Familial hyperprolineamia: report of second case, associated with congenital renal malformation, hereditary hematuria and mild mental retardation, with demonstration of enzyme defect, New Engl. J. Med. 272 (1965) 1243–1254.
[12] M.T. Geraghty, D. Vaughn, A.J. Nicholson, W.W. Lin, G. Jimenez-Sanchez, C. Obie, M.P. Flynn, D. Valle, C.A. Hu, Mutations in the Δ^1-pyrroline-5-carboxylate dehydrogenase gene cause type II hyperprolinemia, Hum. Mol. Genet. 7 (1998) 1411–1415.
[13] H. Jacquet, G. Raux, F. Thibaut, B. Hecketsweiler, E. Houy, C. Demilly, S. Haouzir, G. Allio, G. Fouldrin, V. Drouin, J. Bou, M. Petit, D. Campion, T. Frebourg, PRODH mutations and hyperprolinemia in a subset of schizophrenic patients, Hum. Mol. Genet. 11 (2002) 2243–2249.
[14] J.M. Wood, Genetics of L-proline utilization in *Eschericia coli*, J. Bacteriol. 146 (1981) 895–901.
[15] R. Menzel, J. Roth, Regulation of genes for proline utilization in *Salmonella typhimurium*: autogenous repression by the *putA* gene product, J. Mol. Biol. 148 (1981) 21–44.
[16] S. Maloy, J.R. Roth, Regulation of proline utilization in *Salmonella typhimurium*: characterization of *put*:Mu L(Ap, *lac*) operon fusions, J. Bacteriol. 154 (1983) 561–568.
[17] P. Ostrovsky De Spicer, K. O'Brian, S. Maloy, Regulation of proline utilization in *Salmonella typhimurium*: a membrane-associated dehydrogenase binds DNA in vitro, J. Bacteriol. 173 (1991) 211–219.
[18] C.C. Chen, T. Tsuchiya, Y. Yamane, J.M. Wood, T.H. Wilson, J. Membr. Biol. 84 (1985) 157–164.
[19] J. Wood, Membrane association of proline dehydrogenase in *Escher-*

ichia coli is redox dependent, Proc. Natl. Acad. Sci. U. S. A. 84 (1987) 373–377.
[20] A.M. Muro-Pastor, P. Ostrovsky, S. Maloy, Regulation of gene expression by repressor localization: biochemical evidence that membrane and DNA binding by the PutA protein are mutually exclusive, J. Bacteriol. 179 (1997) 2788–2791.
[21] M.W. Surber, S. Maloy, Regulation of flavin dehydrogenase compartmentalization: requirements for PutA-membrane association in *Salmonella typhimurium*, Biochim. Biophys. Acta 1421 (1999) 5–18.
[22] E.D. Brown, J.M. Wood, Conformational change and membrane association of the PutA protein are coincident with reduction of its FAD cofactor by proline, J. Biol. Chem. 268 (1993) 8972–8979.
[23] D.F. Becker, E.A. Thomas, Redox properties of the PutA protein from *Escherichia coli* and the influence of the flavin redox State on PutA–DNA interactions, Biochemistry 40 (2001) 4714–4722.
[24] M.P. Vinod, P. Bellur, D.F. Becker, Electrochemical and functional characterization of the proline dehydrogenase domain of the PutA flavoprotein from *Escherichia coli*, Biochemistry 41 (2002) 6525–6532.
[25] Y.H. Lee, S. Nadaraia, D. Gu, D.F. Becker, J.J. Tanner, Structure of the proline dehydrogenase domain of the multifunctional PutA flavoprotein, Nat. Struct. Biol. 10 (2003) 109–114.
[26] W. Zhu, Y. Gincherman, P. Docherty, C.D. Spilling, D.F. Becker, Effects of proline analog binding on the spectroscopic and redox properties of PutA, Arch. Biochem. Biophys. 408 (2002) 131–136.
[27] H. Lineweaver, D. Burk, J. Am. Chem. Soc. 56 (1934) 658.
[28] M. Dixon, The determination of enzyme inhibitor constants, Biochem. J. 55 (1953) 170–171.
[29] M. Dixon, The effect of pH on the affinities of enzymes for substrates and inhibitors, Biochem. J. 55 (1953) 161–170.
[30] W.W. Cleland, The use of pH studies to determine chemical mechanisms of enzyme-catalyzed reactions, Methods Enzymol. 87 (1982) 390–405.
[31] M.T. Stankovich, An anaerobic spectroelectrochemical cell for studying the spectral and redox properties of flavoproteins, Anal. Biochem. 109 (1980) 295–308.
[32] P. Hemmerich, V. Massey, Flavin and 5-deazaflavin: a chemical evaluation of 'modified' flavoproteins with respect to the mechanisms of redox biocatalysis, FEBS Lett. 84 (1977) 5–21.
[33] W. Zhu, D.F. Becker, Flavin redox state triggers conformational changes in the PutA protein from *Escherichia coli*, Biochemistry 42 (2003) 5469–5477.
[34] C.M. Harris, L. Pollegioni, S. Ghisla, pH and kinetic isotope effects in D-amino acid oxidase catalysis, Eur. J. Biochem. 268 (2001) 5504–5520.
[35] S. Umhau, L. Pollegioni, G. Molla, K. Diederichs, W. Welte, M.S. Pilone, S. Ghisla, The X-ray structure of D-amino acid oxidase at very high resolution identifies the chemical mechanism of flavin-dependent substrate dehydrogenation, Proc. Natl. Acad. Sci. U. S. A. 97 (2000) 12463–12468.
[36] C. Binda, A. Mattevi, D.E. Edmondson, Structure–function relationships in flavoenzyme-dependent amine oxidations, J. Biol. Chem. 277 (2002) 23973–23976.
[37] Z. Zhou, R.P. Swenson, Electrostatic effects of surface acidic amino acid residues on the oxidation–reduction potentials of the flavodoxin from *Desulfovibrio vulgaris* (Hildenborough), Biochemistry 34 (1995) 3183–3192.
[38] K. Maeda-Yorita, G.C. Russell, J.R. Guest, V. Massey, C.H.J. Williams, Modulation of the oxidation–reduction potential of the flavin in lipoamide dehydrogenase from *Escherichia coli* by alteration of a nearby residue, K53R, Biochemistry 33 (1994) 6213–6220.
[39] F. Talfournier, A. Munro, J. Basran, M.J. Sutcliffe, S. Daff, S.K. Chapman, N.S. Scrutton, α-Arg237 in *Methylophilus methylotrophus* (sp. W3A1) electron-transferring flavoprotein affords ~200-millivolt stabilization of the FAD anionic semiquinone and a kinetic block on full reduction to the dihydroquinone, J. Biol. Chem. 276 (2001) 20190–20196.